JGP Journal of General Physiology

RESEARCH ARTICLE

Sarcomere length–dependent effects on Ca^{2+}-troponin regulation in myocardium expressing compliant titin

King-Lun Li[1], Mei Methawasin[3], Bertrand C.W. Tanner[2], Henk L. Granzier[3], R. John Solaro[4], and Wen-Ji Dong[1,2]

Cardiac performance is tightly regulated at the cardiomyocyte level by sarcomere length, such that increases in sarcomere length lead to sharply enhanced force generation at the same Ca^{2+} concentration. Length-dependent activation of myofilaments involves dynamic and complex interactions between a multitude of thick- and thin-filament components. Among these components, troponin, myosin, and the giant protein titin are likely to be key players, but the mechanism by which these proteins are functionally linked has been elusive. Here, we investigate this link in the mouse myocardium using in situ FRET techniques. Our objective was to monitor how length-dependent Ca^{2+}-induced conformational changes in the N domain of cardiac troponin C (cTnC) are modulated by myosin–actin cross-bridge (XB) interactions and increased titin compliance. We reconstitute FRET donor- and acceptor-modified cTnC(13C/51C)AEDANS-DDPM into chemically skinned myocardial fibers from wild-type and RBM20-deletion mice. The Ca^{2+}-induced conformational changes in cTnC are quantified and characterized using time-resolved FRET measurements as XB state and sarcomere length are varied. The RBM20-deficient mouse expresses a more compliant N2BA titin isoform, leading to reduced passive tension in the myocardium. This provides a molecular tool to investigate how altered titin-based passive tension affects Ca^{2+}-troponin regulation in response to mechanical stretch. In wild-type myocardium, we observe a direct association of sarcomere length–dependent enhancement of troponin regulation with both Ca^{2+} activation and strongly bound XB states. In comparison, measurements from titin RBM20-deficient animals show blunted sarcomere length–dependent effects. These results suggest that titin-based passive tension contributes to sarcomere length–dependent Ca^{2+}-troponin regulation. We also conclude that strong XB binding plays an important role in linking the modulatory effect of titin compliance to Ca^{2+}-troponin regulation of the myocardium.

Introduction

Calcium regulation of cardiac function is a complex process involving multiple components of the sarcomere that affect each other via different feedback mechanisms. Among them, length-dependent activation (LDA) is essential for beat-to-beat regulation of cardiac output and has been considered as the cellular basis underlying the Frank–Starling law of the heart. With LDA, the response of myofilaments to Ca^{2+} becomes more sensitive, and the maximal Ca^{2+}-activated force increases as sarcomere length increases. However, its underlying molecular mechanisms remain elusive (Fukuda et al., 2009; de Tombe et al., 2010; Campbell, 2011; Kobirumaki-Shimozawa et al., 2014). A general consensus is that the LDA likely involves dynamic and complex interplays between a multitude of thick- and thin-filament–based mechanisms (de Tombe et al., 2010; Campbell, 2011), including the sarcomere length–induced changes in the intrinsic properties of the thin filament (Fitzsimons and Moss, 1998; Arteaga et al., 2000; Chandra et al., 2001, 2006; Konhilas et al., 2003; Fuchs and Martyn, 2005; Tachampa et al., 2007; Sun et al., 2009; Farman et al., 2010) and the thick filament (Fuchs and Wang, 1996; Cazorla et al., 2001; Konhilas et al., 2002; Fukuda et al., 2003, 2005; Fuchs and Martyn, 2005; Mateja et al., 2013; Fusi et al., 2016; Piazzesi et al., 2018). Com-

[1]Gene and Linda Voiland School of Chemical Engineering and Bioengineering, Washington State University, Pullman, WA; [2]Integrative Physiology and Neuroscience, Washington State University, Pullman, WA; [3]Department of Cellular and Molecular Medicine, University of Arizona, Tucson, AZ; [4]The Department of Physiology and Biophysics, Center for Cardiovascular Research, College of Medicine, University of Illinois at Chicago, Chicago, IL.

Correspondence to Wen-Ji Dong: dongwenji@wsu.edu.

This work is part of a special collection on myofilament function.

pliance of the giant protein titin (Cazorla et al., 2001; Fukuda et al., 2005; Radke et al., 2007) and the role of myosin binding protein C (Mamidi et al., 2014) are also involved in the sarcomere length dependence of contraction through modulating lattice spacing, thick-filament activation, and interactions between the thin and thick filaments. However, no single mechanism has emerged as the primary determinant of the Frank–Starling relationship.

Among the myofilament proteins, troponin and myosin are two key components involved in the LDA mechanism. Troponin regulates thin-filament activation and cross-bridge (XB) binding in a Ca^{2+}-sensitive manner, and in turn, myosin interacts with actin to form strong XBs to generate force in response to thin-filament activation. The two components are functionally linked through Ca^{2+} binding to the troponin complex and XB feedback, to stabilize or enhance activation along the thin filaments. The Ca^{2+} binding induces an open conformation of the cardiac troponin C (cTnC) N domain (Dong et al., 1999; Li et al., 1999) and leads to interactions between the N domain of cTnC and the C domain of cardiac troponin I (Dong et al., 1999; Li et al., 1999; Hoffman et al., 2006; Xing et al., 2009), which facilitates the shift of tropomyosin from the blocked toward the closed state to promote strong binding of myosin to actin (McKillop and Geeves, 1993; Maytum et al., 1999; Moss et al., 2004). These Ca^{2+}-induced structural transitions in troponin are the molecular basis of regulating thin-filament on/off and XB interactions with the thin filament. Subsequent strong XB binding induces further structural changes in the thin filament that enhance its activation and sensitize it to Ca^{2+} in what is termed "XB feedback" (Gordon and Ridgway, 1987; Güth and Potter, 1987; Hannon et al., 1992; Moss et al., 2004). The XB feedback not only affects troponin regulation but also is believed to play a role in LDA (Moss et al., 2004). In recent studies in skinned cardiac muscle fibers, we used in situ FRET and muscle mechanics to monitor the opening of the N domain of cTnC, as a function of sarcomere length (Rieck et al., 2013; Li et al., 2014). We obtained strong evidence that even at low levels of Ca^{2+}, the actin–myosin interactions exert a significant effect on Ca^{2+} sensitivity and cTnC N-domain opening. Furthermore, when strong XB binding was inhibited by vanadate (Vi), the sarcomere length–dependent effects on the cTnC N-domain opening were eliminated. These results suggest that Ca^{2+}, actin–myosin XB, and sarcomere length all influence the equilibrium between the open and closed conformations of the N domain of cTnC and therefore the on/off equilibrium of thin filament. The technique developed in these studies provides an in situ approach for mechanistic investigation of LDA in cardiac muscle. In this report we present a study using our in situ FRET to examine the role of titin compliance in sarcomere length–dependent modulation of Ca^{2+}-activated troponin regulation.

Titin connects the Z disk to the M band and interacts with both the thick and thin filaments of the cardiac sarcomere. Titin generates passive tension as the cardiac myocyte is stretched, which is positively engaged in LDA, possibly via regulating interfilament lattice spacing (Fukuda et al., 2005, 2010) or straining the thick-filament backbone structure to favor XB interactions (Irving et al., 2011). The relationship between passive tension and sarcomere length can be regulated by modifications of titin spring elements (Trombitás et al., 2000; Wu et al., 2000; Lee et al., 2010) that dominate the passive tension and compliance of titin. For example, a mouse model in which the RNA recognition motif of the titin splicing factor RBM20 is deleted increases the expression of more compliant N2BA titin, and this decreases passive tension and attenuates LDA (Methawasin et al., 2014). A recent time-resolved small-angle x-ray diffraction study on an RBM20 rat model that expresses compliant titin also showed that increased titin compliance reduces myofilament LDA (Ait-Mou et al., 2016). Evidence suggests that the underlying mechanism involves stretch-induced conformational changes in both the thick-filament and thin-filament proteins, including troponin, that are modulated by titin-based passive tension. However, the molecular basis of how changes in passive tension of titin affect the thin filament, especially troponin, is unknown. To understand the mechanism, we used the in situ FRET technique to monitor how Ca^{2+}-induced conformational change of the N domain of cTnC is modulated by sarcomere length and titin compliance. We compared WT mice and RBM20-deficient mice with increased titin compliance. Findings support that titin-based passive tension modulates sarcomere length-dependent Ca^{2+}-troponin regulation. Furthermore, our results suggest that myosin–actin interaction plays an important role in linking the effect of titin compliance and length-dependent Ca^{2+}-troponin regulation.

Materials and methods

Animal handling protocols

The handling of all the experimental animals followed the institutional guidelines and protocols approved by the Animal Care and Use Committee and the Office of Laboratory Animal Welfare, National Institutes of Health. The muscle fiber studies were approved by the Washington State University Institutional Animal Care and Use Committee.

Preparation of proteins

The recombinant double-cysteine mutant cTnC(T13C/N51C) from rat cDNA clones was subcloned into a pET-3d vector, which was then transformed into BL21(DE3) cells (Invitrogen) and expressed under isopropyl β-D-1-thiogalactopyranoside induction. The expressed proteins were purified as described before (Dong et al., 2007; Rieck et al., 2013; Li et al., 2014; Rieck and Dong, 2014). Our previously established protocol (Dong et al., 2007) was used to modify cTnC(T13C/N51C) with 5-((((2-iodoacetyle)amino) ethyl)amino)naphthalene-1-sulfonic acid (AEDANS) as FRET donor. The diethylaminoethyl column was used to separate unlabeled, singly, and doubly labeled cTnC(T13C/N51C). The singly labeled fraction was collected and divided into two aliquots. One was used as the donor-only sample. The other one was labeled with *N*-(4-dimethylamino-3,5-dinitrophenyl)maleimide (DDPM) at the other cysteine to produce $cTnC(T13C/N51C)_{AEDANS\text{-}DDPM}$, the donor–acceptor sample. The labeling ratio of the donor-only sample was determined spectroscopically using ε_{325} = 6,000 cm^{-1} M^{-1} for AEDANS. Labeling ratios for all protein modification were >95%.

Preparation of pCa solutions

The $-\log_{10}$ of free Ca^{2+} concentration (pCa) solutions were prepared based on calculations of the program by Fabiato (Fabiato and Fabiato, 1979). The high relaxing solution contained (in mM) 50 BES, 30.83 K-propionate, 10 NaN_3, 20 EGTA, 6.29 $MgCl_2$, and 6.09 Na_2ATP. The activating solution (pCa 4.3) contained (in mM) 50 BES, 5 NaN_3, 10 EGTA, 10.11 $CaCl_2$, 6.61 $MgCl_2$, 5.95 Na_2ATP, and 51 K-propionate. Similarly, the relaxing solution (pCa 9.0) was composed of (in mM) 50 BES, 5 NaN_3, 10 EGTA, 0.024 $CaCl_2$, 6.87 $MgCl_2$, 5.83 Na_2ATP, and 71.14 K-propionate. To inhibit XBs, 1 mM sodium Vi was added to the above pCa solutions. To induce ADP-mediated noncycling, strongly bound XBs, ATP in the relaxing and activating solutions was replaced with 5 mM Mg^{2+}-ADP. The ionic strength of all pCa solutions was 180 mM. Protease inhibitors including 5 µM bestatin, 2 µM E-64, 10 µM leupeptin, and 1 µM pepstatin were added to all solutions (Chandra et al., 2007).

Preparation of detergent-skinned cardiac muscle fibers

Mouse cardiac papillary muscle bundles from the left ventricle were dissected in oxygenated HEPES ([in mmol/liter] 133.5 NaCl, 5 KCl, 1.2 NaH_2PO_4, 1.2 $MgSO_4$, 30 2,3-butanedione monoxime, 10 HEPES) solution. Cardiac muscle fibers (~150–200 µm in diameter and 2.0 mm in length) were dissected from the muscle bundles and placed into a relaxing solution ([in mmol/liter] 40 BES, 10 EGTA, 6.56 $MgCl_2$, 5.88 Na-ATP, 1.0 dithiothreitol, 46.35 K-propionate, 15 creatine phosphate, pH 7.0) in presence of 1.0 mM dithiothreitol and 20 mM 2,3-butanedione monoxime. In addition, fresh protease inhibitors including 4 µM benzamidine-HCl, 5 µM bestatin, 2 µM E-64, 10 µM leupeptin, 1 µM pepstatin, and 200 µM phenylmethylsulfonyl fluoride were added to the solution. To ensure the muscle preparations are completely demembranated, the muscle fibers were skinned overnight at 4°C using 1% Triton X-100 in relaxing solution.

Incorporation of fluorescently labeled cTnC(13C/51C)$_{AEDANS\text{-}DDPM}$ constructs into detergent-skinned myocardial fibers

Incorporation of cTnC(13C/51C)$_{AEDANS\text{-}DDPM}$ into mouse skinned myocardial fibers was performed using a modified protocol established for rat myocardium (Rieck et al., 2013; Li et al., 2014). Briefly, endogenous cTnC was extracted in skinned cardiac fibers by incubating fibers in extraction solution for 2.5 h. The extraction solution contained (in mM) 5 trans-1,2-cyclohexanediamine-N,N,N′,N′-tetraacetic acid (CDTA), 40 Tris-HCl (pH 8.4), 0.6 NaN_3, 0.005 bestatin, 0.002 E-64, 0.01 leupeptin, and 0.001 pepstatin. The cTnC extracted fibers were washed with the relaxing solution for 15 min five times. Subsequently, the fibers were incubated overnight in the high relaxing solution containing either 10 µM donor-only or donor–acceptor modified cTnC(T13C/N51C). Protein exchange ratio was examined by performing Western blotting analysis using cTnC-specific antibody (10-T78A; Fitzgerald) as previously described (Rieck et al., 2013; Li et al., 2014). With our exchange protocol, >80% of endogenous cTnC was replaced with fluorescently labeled cTnC constructs. The Ca^{2+}-activated maximal tension was measured in pCa 4.3 solution for cTnC extracted and exogenous cTnC reconstituted fibers to determine the residual tension and maximum tension recovery, respectively.

Simultaneous measurement of isometric force and time-resolved fluorescence intensity in detergent-skinned cardiac muscle fibers

Simultaneous measurements of isometric force and time-resolved fluorescence intensity were conducted according to a protocol previously described (Rieck et al., 2013; Li et al., 2014). All the measurements were made using the Güth Muscle Research System modified with a TBX picosecond photon detection module (HORIBA Jobin Yvon). Briefly, the skinned muscle fibers reconstituted with fluorescently modified cTnC were attached to the force transducer (KG7A; SI Heidelberg) and a stationary tweezer. The sarcomere length of the fiber was adjusted to either 1.8 or 2.2 µm using laser diffraction. Fibers were subjected to an initial cycle of activation and relaxation, and sarcomere length was readjusted if necessary. Half of our measurements started at 1.8 µm sarcomere length, whereas the other half started at 2.2 µm sarcomere length. The experimental temperature of the pCa solution was controlled at 20 ± 0.2°C using a bipolar temperature controller (TC2BIP; Cell MicroControls) coupled with a cooling/heating module (CH; Cell MicroControls). Fluorescence intensity decays were obtained using excitation at 340 nm from a NanoLED (N-340; HORIBA Jobin Yvon) with a <1.2-ns pulse width and a 500-nm cutoff filter. During steady-state activation, tension and time-resolved measurements were synchronously recorded as described previously (Rieck et al., 2013; Li et al., 2014). The fluorescence intensity decays were processed and recorded by a FluoroHub-B (HORIBA Jobin Yvon) using time-corrected single photon counting technology. Typically, a total of 10,000 photon counts at peak channel, at which each decay starts, was collected in 1–1.5 min. Fig. 1 demonstrates a typical fluorescence intensity decay (Fig. 1 A) with residue and autocorrelation analysis, and tension (Fig. 1 B) measured at 1.8 µm sarcomere length. The mean distances (r) describing the relative distances between donor and acceptor sites within the cTnC population under different conditions were derived from the decays. These measurements were performed repeatedly in the presence of cycling XBs (5 mM Mg-ATP); Mg^{2+}-ADP-induced noncycling, strong-binding XBs (5 mM Mg-ADP + 0 mM ATP); and vanadate-induced noncycling, weak-binding XBs (1 mM Vi + 5 mM Mg-ATP).

Determination of interprobe distances from measured fluorescence intensity decays

The AEDANS–DDPM interprobe distance distribution associated with a specific test condition was determined as previously described (Li et al., 2016). The AEDANS excited-state decays obtained from the donor-only samples were fitted with a multiexponential function (Liao et al., 1992):

$$I_D(t) = \sum_{i=1}^{n} \alpha_i \, e^{-t\tau_i^{-1}}, \quad (1)$$

where α_i represents the fractional amplitude associated with each correlation time τ_i that contributes to the overall excited-state decay process. The AEDANS excited-state decays obtained from the donor–acceptor samples were fit to the following

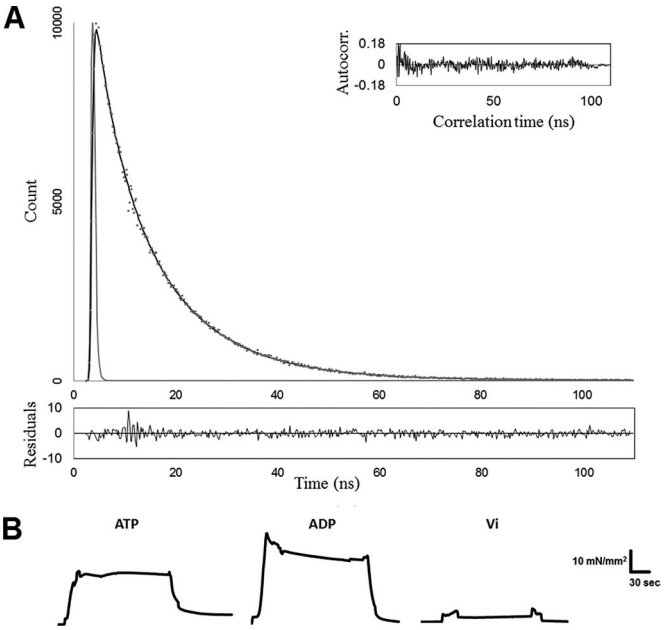

Figure 1. **Simultaneous measurements of time-resolved fluorescence lifetime and contractile force were performed in skinned cardiac muscle preparation reconstituted with fluorescently labeled cTnC(13c/51c)$_{AEDANS\text{-}DDPM}$. (A)** Top: A representative trace of the fluorescence lifetime decay in the presence of acceptor DDPM (gray dots), which was measured at sarcomere length 2.2 µm in the absence of Ca^{2+} (pCa 9.0). The decay was fit to Eq. 1 (black line). The autocorrelation (inset) and residual (bottom) were used to judge the goodness of fit. **(B)** Isometric tension was measured under different XB states (as indicated above the force traces). The magnitudes of tension and time are presented by the vertical and horizontal scale bars, respectively.

equation using DecayFit 1.4 (Fluorescence Decay Analysis Software; FluorTools):

$$I_{DA}(t) = \frac{\int_0^\infty P(r)\left(\sum_{i=1}^{n}\alpha_{D_i}\, e^{-\frac{t}{\tau_{D_i}}\left(1+\left(\frac{R_0}{r}\right)^6\right)}\right)dr}{\int_0^\infty P(r)\,dr}, \quad (2)$$

where r is the distance between the donor and acceptor fluorophores; α_{Di} and τ_{Di} are the fractional amplitude and correlation time parameters, respectively, determined for AEDANS in the absence of acceptor; and R_o is the Förster critical distance at which energy transfer is 50% efficient, which was calculated from the spectral properties of AEDANS and DDPM (Dong et al., 1999). The probability distribution of interprobe distances is $P(r)$, and in this study we assume it to be a single Gaussian as follows:

$$P(r) = \frac{1}{Z\sigma\sqrt{2\pi}}\, e^{-\frac{1}{2}\left(\frac{r-\bar{r}}{\sigma}\right)^2}, \quad (3)$$

where $\bar{r}$ is the mean distance and σ is the standard deviation of the distribution; $P(r)$ is normalized by area, and Z is the normalization factor.

Statistical data analysis

A two-way ANOVA was used to analyze the contractile and conformational parameters. The factors in the analysis include (a) titin variant (WT and RBM20) and (b) sarcomere length (1.8 or 2.2 µm). Post hoc tests (planned multiple pairwise comparisons) were made using uncorrected Fisher's least significant difference method after the analyses of two-way ANOVA. Comparisons were made to determine the effects of titin variant and sarcomere length on contractile and conformational parameters. Fitted values of $\bar{r}$ are reported as mean ± SEM with statistical significance level set at *, $P < 0.05$, or **, $P < 0.01$.

Results

Effects of titin compliance on tension development of skinned myocardial fibers

First, we examined the effects of the increased compliance of titin in RBM20-deficient mice on both Ca^{2+}-independent tension (passive tension) and Ca^{2+}-activated tension (active tension) at different sarcomere lengths. The tension values for the reconstituted WT and RBM20 deletion fibers are shown in Table 1. For the measurements in the relaxed fibers, two-way ANOVA revealed a significant interaction effect under normal cycling XB (ATP) conditions, suggesting that the effects of sarcomere length on Ca^{2+}-independent tension (passive tension) are influenced by the altered compliance of titin. Post hoc multicomparisons showed that an increase in sarcomere length from 1.8 to 2.2 µm caused a significant increase in passive tension of fibers from both WT and RBM20-deficient animals (Fig. 2 A). However, this sarcomere length–dependent passive tension was reduced approximately threefold for in RBM20-deficient mice when compared with WT. When measurements were performed in the activated state, the skinned fibers from both WT and RBM20-deficient mice showed significant increases in Ca^{2+}-activated tension in response to increased sarcomere length (Fig. 2 D). However, the sarcomere length–induced increase in the maximal tension of the RBM20-deficient fibers was less than that of the WT fibers. These observations indicate that increasing compliance of titin blunts sarcomere length effects on both passive tension and maximal Ca^{2+}-activated tension. Table 1 and Fig. 2 also show results in the presence of ADP and the XB inhibitor vanadate (Vi). These additional data show that increased titin compliance significantly reduced the effects of the sarcomere length on tension, regardless of whether muscle is activated or not.

In situ time-resolved FRET measurements of the opening of the N domain of cTnC

To monitor the Ca^{2+}-induced opening of the N domain of cTnC in myocardial fibers, FRET donor and acceptor modified cTnC(13C/51C)$_{AEDANS\text{-}DDPM}$ was reconstituted into chemically skinned muscle fibers. The in situ conformational behaviors of the N domain of cTnC under different conditions were quantitatively characterized using time-resolved FRET measurements. These in situ FRET experiments were designed to evaluate the relationship between the effects of Ca^{2+}-binding to site II of cTnC, XB binding state, and sarcomere length on the conformational change of the N domain of cTnC. The FRET intensity decays of the donor AEDANS, similar to the one shown in Fig. 1 A, acquired under each test condition were analyzed to derive the distribution of the distance between Cys13 and Cys51 using Eq. 3. Parameters from these fits of intensity decays are summarized in Table 2, wherein $\bar{r}$ is the mean distance used to assess the effects of changes in calcium (expressed as pCa), XB binding state, or

Table 1. **Tension values (mean ± SEM) from FRET donor–acceptor reconstituted fibers measured at pCa 9 and 4.3 as a function of XB states and sarcomere lengths**

XB state	pCa	WT tension (mN mm^{-2})			RBM20-deficient tension (mN mm^{-2})		
		1.8 µm SL	2.2 µm SL	*n*[a]	1.8 µm SL	2.2 µm SL	*n*[a]
5 mM ATP	9.0	2.10 ± 0.00	5.50 ± 0.10[b]	8	1.35 ± 0.35[c]	2.10 ± 0.00[b,c]	7
	4.3	20.65 ± 1.55	34.10 ± 0.80[b]		17.65 ± 1.65[c]	26.55 ± 0.55[b,c]	
5 mM ADP[d]	9.0	12.87 ± 2.70	37.30 ± 4.12[b]	8	8.30 ± 0.90	28.03 ± 5.02[b,c]	7
	4.3	17.85 ± 1.95	37.55 ± 0.25[b]		12.85 ± 0.35[c]	26.45 ± 0.35[b,c]	
1 mM Vi[e]	9.0	2.05 ± 1.55	8.90 ± 0.30[b]	6	1.40 ± 1.20	5.20 ± 1.30[b,c]	6
	4.3	2.35 ± 0.15	11.90 ± 0.50[b]		1.75 ± 0.55	7.45 ± 0.85[b,c]	

pCa, $-\log_{10}$ of free Ca^{2+} concentration; SL, sarcomere length.
[a]Number of fibers used in each set of measurements.
[b]Compared with 1.8 µm sarcomere length at each condition ($P < 0.05$).
[c]Compared with WT at the same cross-bridge condition, sarcomere length, and Ca^{2+} activation state ($P < 0.05$).
[d]ATP was absent in ADP solutions.
[e]Vi solutions also contained 5 mM ATP.

sarcomere length on the conformational change of the N domain of cTnC. Also summarized in Table 2 are the full width at half maximum (FWHM) of the distance distributions, a parameter closely correlated with the dynamic information associated with the structure monitored by FRET. A large FWHM derived from FRET decays suggests a dynamic/flexible structure, whereas a small FWHM suggests a relatively rigid structure.

Tables 1 and 2 and Fig. 3 show maximal activation of the reconstituted myocardial fibers from WT mice under normal ATP condition. Results show an increase in the mean distance between residues Cys13 and Cys51 in the N domain of cTnC and that the increase is sarcomere length dependent. As sarcomere length increased from 1.8 to 2.2 µm, the mean distance increased by 0.9 and 1.9 Å for the relaxed (pCa 9.0) and activated states (pCa 4.3), respectively. When the measurements were performed in the presence of strong XB (ADP state) conditions, increasing sarcomere increased the mean distance by 1.2 and 1.7 Å for the relaxed (pCa 9.0) and activated states (pCa 4.3), respectively. These changes were accompanied by increases in FWHM (Table 2), suggesting more flexible cTnC N-domain conformation as sarcomere length increases. When the strong XB formation was inhibited by vanadate (Vi state), the sarcomere length–induced increase in the mean distance was significantly attenuated (Fig. 3 and Table 2). These results suggest that the Ca^{2+}-induced conformational change of the N domain of cTnC, which is directly linked to cardiac thin-filament regulation, is sensitive to sarcomere length and that the sarcomere length–dependent conformational changes of the N domain of cTnC are closely associated with the conformational state of bound XBs. The strong actin–myosin interaction is important to convert the effect of sarcomere length to the troponin regulation.

Effects of compliance of titin on the SL-dependent behavior of the N domain of troponin C

To examine potential effects of titin compliance on the conformational behavior of the N domain of cTnC, similar in situ FRET measurements were performed with chemically skinned myocardial fibers from RBM20-deficient mice, which were reconstituted with $cTnC(13C/51C)_{AEDANS\text{-}DDPM}$. The measurements were performed at different sarcomere lengths under various conditions. The distances between residues Cys13 and Cys51 derived from FRET decays are given in Table 2 and Fig. 3. Two-way ANOVA showed significant interaction effects under the ATP conditions for both the relaxed (pCa 9.0) and activated (pCa 4.3) states. Analysis showed that the increased titin compliance diminished the sarcomere length–induced increases in N-cTnC opening that were observed in WT fibers in both relaxed and Ca^{2+}-activated muscle (Fig. 3 A). Similarly, significant interaction effects were found under ADP conditions, whether or not the fibers were activated by Ca^{2+}. Post hoc multicomparisons showed significant differences in the sarcomere length–induced conformational changes of N-cTnC between the WT group and the RBM20-deficient group (Fig. 3 B). When strong force-generating XBs were inhibited by Vi, the interaction effects of the compliance of titin on the sarcomere length–induced conformation change of N-cTnC were blunted (Fig. 3 C). These results suggest that increasing titin compliance attenuates the effect of sarcomere length on the N-cTnC conformation in the presence of strong actin–myosin interactions.

Effects of titin compliance on the XB-dependent behavior of the N domain of troponin C

The interplay between titin compliance, XB state, sarcomere length, and N-cTnC conformation was studied in further detail. We examined the sarcomere length effects on the XB-dependent conformational changes of N-cTnC in response to varied titin compliance. Fig. 4 shows that for the WT group, the strong interaction between myosin and actin dominated under ADP conditions, exhibiting a greater effect on the N-cTnC opening at both sarcomere lengths compared with the ATP state. The ADP effects could be observed regardless of the myofilament Ca^{2+} activa-

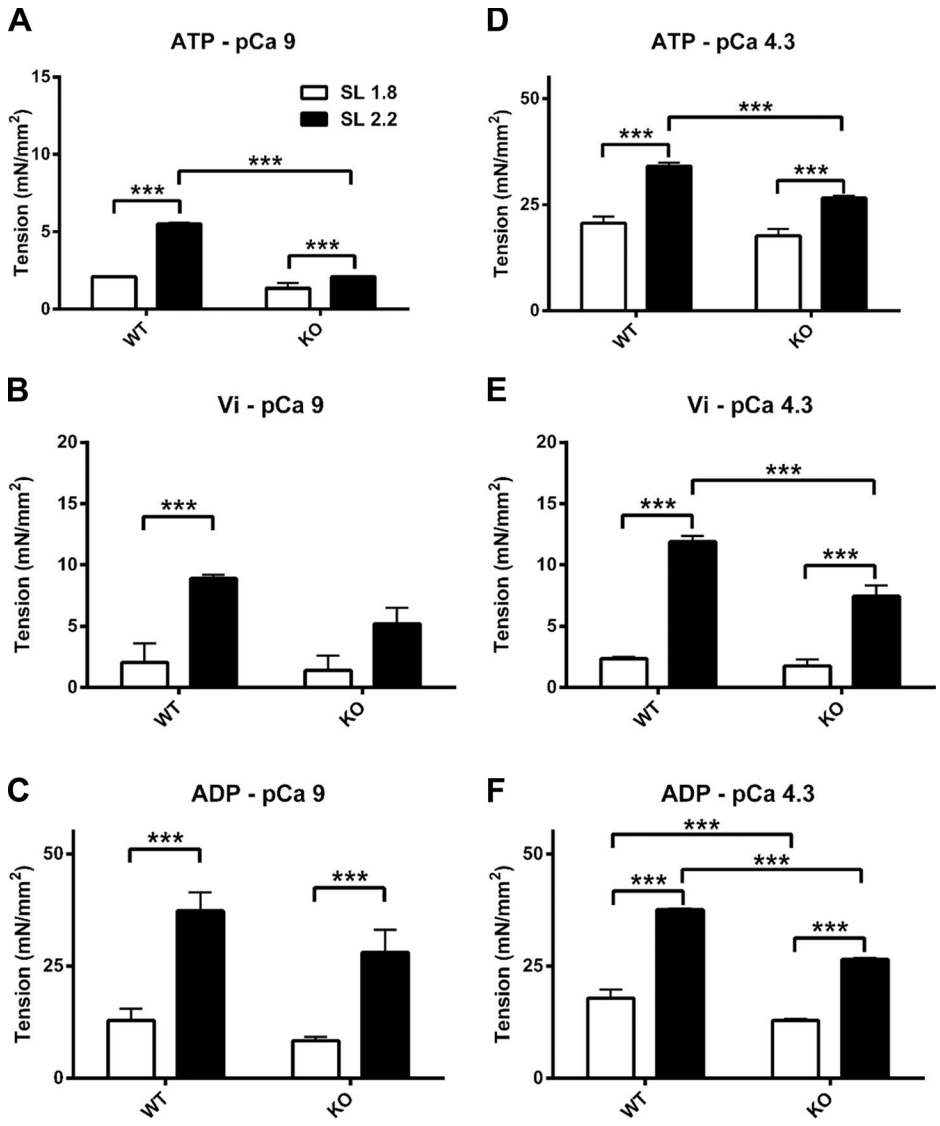

Figure 2. **Effects of XB state on isometric tension at 1.8 µm (unfilled bar) and 2.2 µm (filled bar). (A–C)** Isometric tension measured at pCa 9. **(D–F)** Tension measured at pCa 4.3. Note that the scales of y axis (tension) are different for each graph. To examine the effects of XB state on tension development, tension measurements were made in the presence of 5 mM ATP (A and D), 5 mM ADP (C and F), and 1 mM Vi (B and E). Values are reported as mean ± SEM. ***, $P < 0.01$.

tion level, although the magnitudes of the effects were greater under the Ca^{2+}-activated state (Fig. 4 B) versus the relaxed state (Fig. 4 A). However, the sarcomere length–dependent ADP-induced increases in the N-cTnC opening observed in the WT group were significantly attenuated in RMB20-deficient fibers. This suggests that one of the roles of titin compliance in myofilament regulation may be related to modulation of the myosin–actin XB interaction, which further affects troponin regulation via XB feedback mechanisms.

Effects of titin compliance on Ca^{2+}-induced N domain of troponin C opening at sarcomere length of 1.8 and 2.2 µm

Because thin-filament regulation is directly related to Ca^{2+}-induced N-cTnC conformational changes, we also examined the effects of titin compliance on the Ca^{2+}-induced conformation changes of N-cTnC under various XB states. The Ca^{2+}-induced changes in N-cTnC conformation were represented by the distance change (Δr) between the Ca^{2+}-bound state and the relaxed state (Fig. 5). Two-way ANOVA revealed significant interaction effects under ATP conditions. Post hoc multicomparisons showed a significant sarcomere length–dependent Ca^{2+}-induced N-cTnC opening for the WT fibers. Fig. 5 shows that the Δr of the N-cTnC opening increased from 8.7 to 9.7 Å as the sarcomere length of the WT group changed from 1.8 to 2.2 µm. However, this sarcomere-dependent opening was blunted in the RBM20-deficient group. A similar trend was seen under ADP conditions, in which the titin RBM20 deletion also blunted the sarcomere length dependence of the Ca^{2+}-induced N-cTnC opening (from 10.8 to 11.5 Å). No significant interaction effect was found under Vi conditions. Regardless of sarcomere length and titin background, Ca^{2+}-induced N-cTnC opening remained the same in the presence of Vi. These observations demonstrated that under conditions that promote force-generating XBs, titin may have allosteric effects on Ca^{2+}-cTnC regulation.

Table 2. **Distance distributions observed in cTnC(13c/51c)$_{AEDANS-DDPM}$ reconstituted fibers under different biochemical conditions**

XB state	pCa	WT				n^a	Titin RBM20				n^a
		1.8 µm SL		2.2 µm SL			1.8 µm SL		2.2 µm SL		
		r^b (Å)	FWHM^c (Å)	r^b (Å)	FWHM^c (Å)		r^b (Å)	FWHM^c (Å)	r^b (Å)	FWHM^c (Å)	
5 mM ATP	9.0	12.98±0.24	5.83± 0.29	13.83 ± 0.25§	7.19 ± 0.26§	8	12.45 ± 0.32	5.72 ± 0.62	12.95 ± 0.45	5.82 ± 0.51	7
	4.3	21.67±0.17	6.50± 0.37	23.51 ± 0.31§§	8.91± 0.68§§		21.01 ± 0.39	4.68 ± 0.73	21.50 ± 0.35†	5.27 ± 0.36††	
5 mM ADP[d]	9.0	13.70±0.24	5.92± 0.25	14.87± 0.23§*	6.82± 0.27§	8	13.04 ± 0.34	5.81 ± 0.32	13.68 ± 0.49†	5.60 ± 0.28†	7
	4.3	24.46±0.23	5.72± 0.59	26.34± 0.36§§**	6.30 ± 0.37**		22.27 ± 0.66††*	4.57 ± 0.42	23.11 ± 0.55††**	4.77 ± 0.36†	
1 mM Vi[e]	9.0	12.03±0.46	5.43± 0.28	12.94 ± 0.33	5.53 ± 0.38**	6	11.82 ± 0.44	6.03 ± 0.33	11.75 ± 0.39	5.92 ± 0.25	6
	4.3	20.09±0.45	5.82± 0.47	21.51 ± 0.57§*	5.95 ± 0.42**		20.28 ± 0.86	5.81 ± 0.35	20.40 ± 0.45†*	6.28 ± 0.38**	

Absolute parameter values are given as mean ± SEM. Statistical significance level set at P < 0.05 (§, †, and *) and P < 0.01 (§§, ††, and **) for the following: §, comparing to 1.8 µm sarcomere length at each condition; †, comparing to WT at the same cross-bridge condition, sarcomere length, and Ca^{2+} activation state; and *, comparing to ATP condition at the same sarcomere length and Ca^{2+} activation state. pCa, $-\log_{10}$ of free Ca^{2+} concentration; SL, sarcomere length.

[a]Number of fibers used in each set of measurements.

[b]*r* is the mean distance associated with the distribution.

[c]FWHM denotes the full width at half maximum.

[d]ATP was absent in ADP solutions.

[e]Vi solutions also contained 5 mM ATP.

Discussion

The I-band region of titin functions as a molecular spring that develops passive tension during diastole when sarcomeres are stretched (Granzier and Labeit, 2006). The level of titin-based passive tension can be altered via differential splicing, resulting in titin isoforms (N2BA and N2B titin) with spring segments that vary in length (Wu et al., 2000). In the left ventricle, the isoforms are coexpressed at the level of the half-sarcomere (Trombitás et al., 2001), and in human myocardium the two isoforms are expressed at approximately equal levels. It has been shown that the expression ratio is significantly increased toward the compliant N2BA isoform in various cardiac diseases, including ischemic heart disease (Neagoe et al., 2002) and dilated cardiomyopathy (Nagueh et al., 2004). Thus, research to better understand how titin compliance affects myofilament force regulation is warranted. The main objective of our study was to test the hypothesis that an alteration in titin compliance affects Ca^{2+}-troponin regulation through strong XB attachment. Our results support this hypothesis and advance understanding of the molecular basis of the Frank–Starling relation.

It is well known that length-dependent increases in the maximal force and Ca^{2+} sensitivity of force regulation are major characteristics of LDA. Our force measurements showed a robust sarcomere length–induced increase in passive tension and maximal active tension of skinned myocardial fibers from mouse tissues regardless of the XB state (i.e., under ATP, ADP, or Vi conditions [Fig. 2, A–C]). When titin compliance is increased, passive tension and active force at each XB state are significantly blunted compared with WT samples; however, the length-dependent effects on tension development are not significantly altered (Table 1 and Fig. 2, D and E). These results suggest that increasing titin compliance does not have a major effect on length-dependent tension (maximal tension values). These observations are consistent with our previous study with skinned myocardium from RBM20-deficient mice, which also showed that increased titin compliance had only a minor effect on the length-dependent increase in maximal active tension (Pulcastro et al., 2016). Even though no length-dependent effects on maximal activated tension relationship of WT and RBM20 deletion myocardium are presented in this current report, our prior studies examined Ca^{2+} sensitivity of LDA in these same RBM20 deletion mice. This prior study clearly showed that increased titin compliance abolished the length-dependent increase of Ca^{2+} sensitivity that is present in WT myocardium (Pulcastro et al., 2016). Sarcomere length–induced Ca^{2+} sensitivity change is a major component of LDA effect and appears to depend on titin compliance. The observed weak correlation between the sarcomere length–induced change in maximal tension and the change in Ca^{2+} sensitivity may indicate additional mechanism underlying sarcomere length–induced change in myocardial Ca^{2+} sensitivity, for example, the change in thin-filament length. Even though thin-filament length is known to vary with sarcomere length, it is unlikely the mechanism revealed here involves thin-filament length changes considering the fact that increased titin compliance decreased Ca^{2+} sensitivity as shown in our previous study (Pulcastro et al., 2016). Moreover, thin-filament length was not altered by varying size of titin as

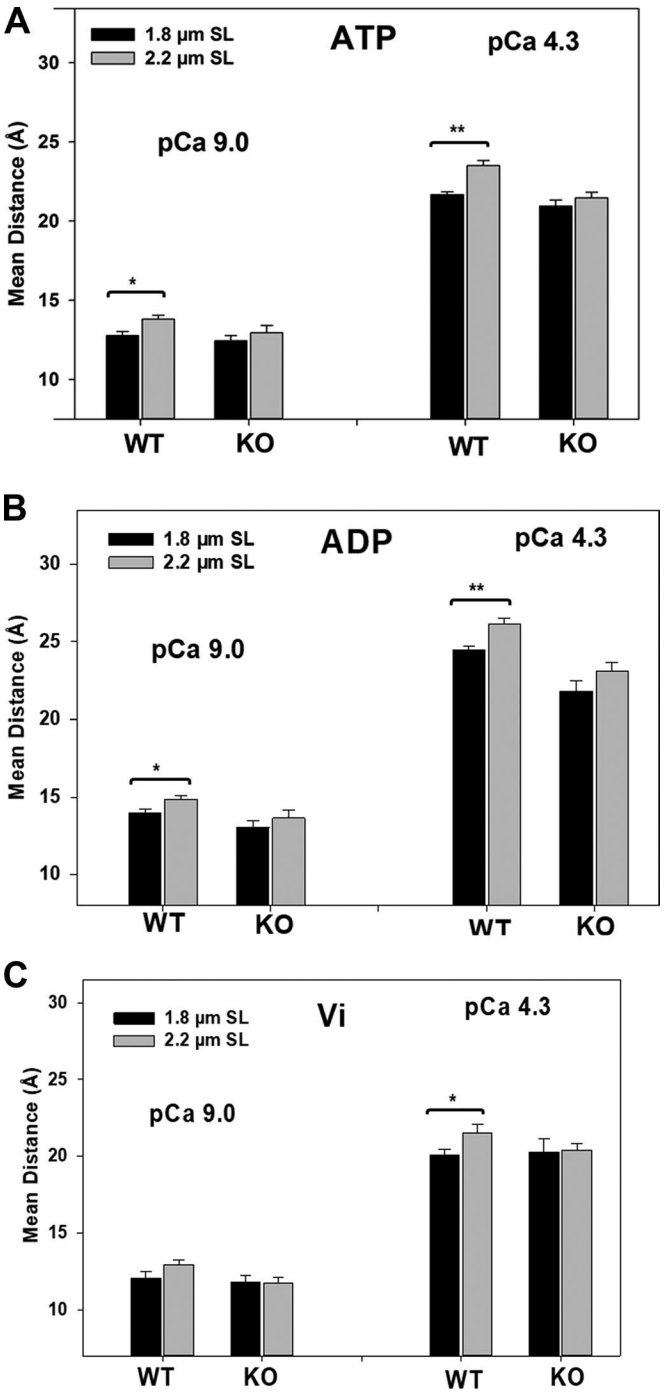

Figure 3. **Sarcomere length effects on structural conformation of the N domain of cTnC under different Ca^{2+} activations and XB conditions.** Distance recovered from cTnC(13c/51c)$_{AEDANS-DDPM}$ reconstituted cardiac muscle preparations from WT and RBM20 knockout (KO) groups at 1.8 μm (black bar) and 2.2 μm (gray bar). **(A–C)** The measurements were performed at pCa 9 and pCa 4.3 under XB conditions in the presence of 5 mM ATP (A), 5 mM ADP (B), and 1 mM Vi (C). Parameter values are reported as mean ± SEM. *, $P < 0.05$; **, $P < 0.01$.

shown by Granzier's group (Kolb et al., 2016). Since Ca^{2+} sensitivity is closely associated with thin-filament regulation, as well as with thick-filament activation (Gordon and Ridgway, 1987; Güth and Potter, 1987; Hannon et al., 1992; Moss et al., 2004; Linari et al., 2015), these results indicate that a major role of the titin in LDA may involve titin strain–dependent effects on protein–protein interactions within both thick filament and thin filament, as suggested by a recent time-resolved small-angle x-ray diffraction study by De Tombe and colleagues (Ait-Mou et al., 2016; see discussion below).

To explore how titin might affect thin-filament regulation, we focus on sarcomere length–dependent Ca^{2+}-troponin regulation in response to altered titin compliance. Under normal XB cycling conditions (ATP), the sarcomere length–dependent tension development observed in WT fibers was accompanied by enhanced Ca^{2+}-troponin regulation, represented by the N-cTnC conformational change (Fig. 3 A) and Ca^{2+}-induced opening (Fig. 5). Sarcomere length–dependent enhancement of Ca^{2+}-troponin regulation was found to be associated with both cycling (under ATP conditions) and strongly bound XBs (under ADP conditions; Figs. 3, A and B, and 5), whereas inhibited force generation and cycling XBs by Vi significantly attenuates these effects (Figs. 3 C and 5). The sarcomere length change was able to exert a significant effect on cTnC N-domain opening, even at a relaxing level of Ca^{2+} (Table 2). When measurements were performed with skinned myocardial fibers from RBM20-deficient mice, these length-dependent enhancements of Ca^{2+}-induced conformational changes in N-cTnC were blunted (Figs. 3 and 5). These results support that titin-based passive tension is indeed involved in sarcomere length–modulated Ca^{2+}-troponin regulation, and it is likely that the modulatory effect of titin compliance is transduced to Ca^{2+}-troponin regulation through force-generating myosin–actin interactions.

It is known that a change in sarcomere length may result in a change in the cTnC affinity (Feest et al., 2014) and the equilibrium of myosin–actin interactions (Fuchs and Wang, 1997). The interplay between Ca^{2+}-troponin regulation and myosin–actin interaction may play a role in the LDA of the myocardium. The RBM20 deletion that reduced N-cTnC conformational changes observed under normal cycling and strong XB conditions in this study may be related to the low Ca^{2+} sensitivity of the RBM20 myocardium (Pulcastro et al., 2016). Consequently, it is plausible that the reduced Ca^{2+}-induced conformational change of N-cTnC would affect the overall force production of myocardium by regulating the equilibrium of myosin–actin interaction, as shown in Fig. 2, where force production was reduced by 20% in fibers with the RBM20 deletion. We also note that the mechanism by which sarcomere length affects Ca^{2+}-troponin regulation of RBM20 myocardium primarily involves the strong myosin–actin interaction to modulate Ca^{2+}-troponin regulation via XB feedback (Fitzsimons and Moss, 1998; Smith et al., 2009). Compared with normal XB cycling (ATP state; Fig. 4), the strong myosin–actin interaction (ADP state) exhibited stronger effects on the conformation of N-cTnC at both sarcomere lengths—regardless of Ca^{2+} activation state—yet these effects were attenuated by increased titin compliance. These results provide evidence that titin compliance is directly involved in modulating strong myosin–actin interactions, which can then affect myofilament regulation by influencing the thin-filament on/off equilibrium due to XB feedback.

The observations that the conformation of N-cTnC in the WT group can be affected by strong XB binding (Fig. 4 A) and sarco-

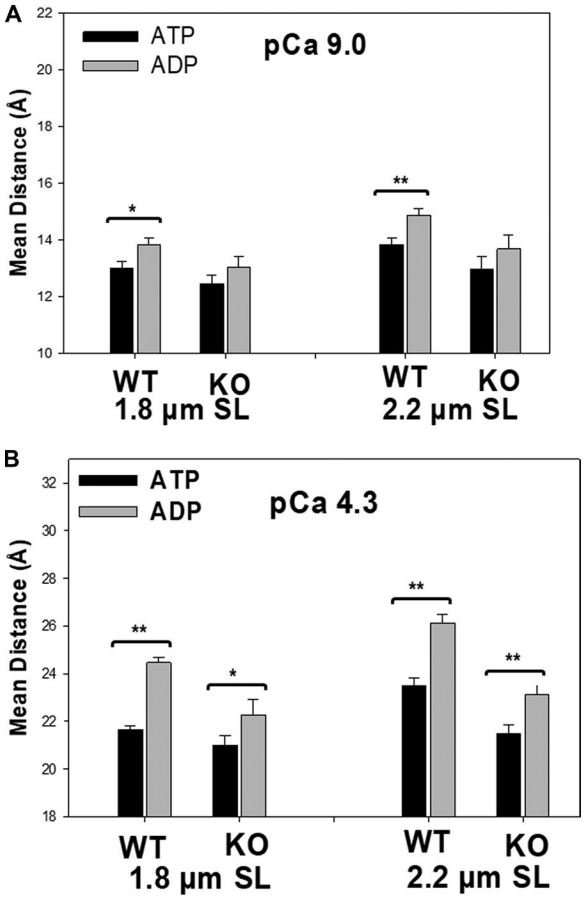

Figure 4. **Strong XB effects on structural conformation of the N domain of cTnC under different Ca^{2+} activation states.** Distance recovered from $cTnC(13c/51c)_{AEDANS\text{-}DDPM}$ reconstituted cardiac muscle preparations from WT and RBM20 knockout (KO) groups at 1.8 µm (black bar) and 2.2 µm (gray bar). **(A and B)** The measurements were performed at pCa 9 (A) and pCa 4.3 (B) and in the presence of 5 mM ATP and 5 mM ADP, respectively. Values are reported as mean ± SEM. *, P < 0.05; **, P < 0.01.

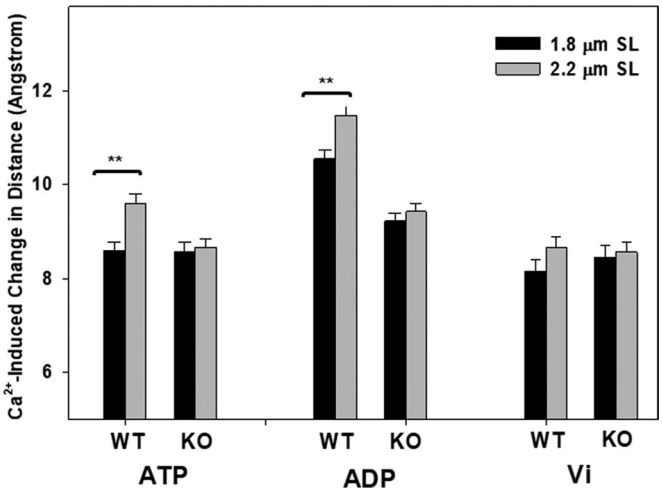

Figure 5. **Effects of sarcomere length on Ca^{2+}-induced N-cTnC opening under different XB conditions.** Distance change represents the magnitude of N-cTnC opening induced by Ca^{2+}, which is the difference in distance between pCa 9 and pCa 4.3. The magnitude of N-cTnC opening was measured for WT and RBM20 knockout (KO) groups at 1.8 µm (black bar) and 2.2 µm (gray bar) in the presence of 5 mM ATP, 5 mM ADP, and 1 mM Vi. Values are reported as mean ± SEM. **, P < 0.01.

mere length (Fig. 3) under relaxed conditions (pCa 9.0) are intriguing. It is known that at relaxed pCa levels, the strong interaction between cardiac troponin I and actin filament anchors tropomyosin in the blocked state to inhibit the interaction between myosin and actin (i.e., the XB interaction occurs only when myofilaments are activated by Ca^{2+} binding to troponin; McKillop and Geeves, 1993; Maytum et al., 1999; Moss et al., 2004). However, our results demonstrate that the presence of ADP, which promotes strong XB interactions regardless of Ca^{2+} activation, can lead to a more open conformation of N-cTnC when the myocardial fiber is at relaxed state. This observation is consistent with the results reported previously (Rieck et al., 2013; Li et al., 2014). This phenomenon has been designated as "a myosin-induced open state," which is suggested to play a role in elevating the basal myofilament activity and competing with the normal Ca^{2+}-activated pathway during myofilament regulation (Lehrer, 2011; Lehrer and Geeves, 2014). Although the mechanism of this myosin-induced effect remains elusive, it may be closely related to the observed sarcomere length effect at the relaxed state (Fig. 3).

Our results corroborate two recent studies in the field. One was from Sun's group, in which fluorescence polarization was used to monitor conformational changes in troponin in the thin filament and in the myosin regulatory chain in the thick filament in response to sarcomere length change (Zhang et al., 2017). The results revealed that the troponin conformation can be altered by sarcomere stretch when the strong myosin–actin interaction is inhibited. The other study was from de Tombe's group, in which time-resolved small-angle x-ray diffraction and fluorescence were used to investigate how titin strain affects sarcomere length–dependent structural changes of both thin-filament and thick-filament proteins (Ait-Mou et al., 2016). The x-ray diffraction measurements revealed significant changes in the reflections of myosin and troponin upon muscle stretch in the relaxed state, and fluorescence measurement confirmed the sarcomere length–induced changes in troponin conformation in relaxed cardiac muscle cells. These sarcomere length–dependent changes in the intensities of the myosin/troponin-based x-ray reflections were greatly reduced in myocardium from transgenic rats expressing a giant splice isoform of titin, suggesting that titin-based passive tension mediates the sarcomere length effect on thin-/thick-filament structure. It is noted that another recent x-ray study of muscle did not find an effect of sarcomere stretch on the intensity of the troponin-based reflection (T3; Reconditi et al., 2017). Further studies are needed to resolve the discrepancy between these two x-ray studies.

These results discussed above provide evidence directly linking the mechanical stretch of the myocardium to the conformation of troponin C. Our current study shows that the effect is reduced when titin becomes more compliant (Fig. 3). However, what is the mechanism by which titin compliance exerts such an effect? We speculate that multiple mechanisms may be involved. One possibility is the direct structural effect of sarcomere length on troponin conformation. However, the stretch-induced struc-

tural arrangement of troponin observed by de Tombe's group (Ait-Mou et al., 2016) is quite different from the structural change of troponin induced by Ca^{2+} binding to N-cTnC in myocardium. Therefore, it is unlikely that the altered titin compliance can directly influence the Ca^{2+}-induced change of troponin. Another mechanism may involve the sarcomere length–dependent myosin-induced effect on troponin conformation discussed earlier (Lehrer, 2011; Lehrer and Geeves, 2014). Increasing titin compliance potentially may alter the energies of interaction involved in the strong XB feedback interaction with troponin. Increased titin compliance may also diminish the super relaxed to disordered relaxed transition due to lower passive force levels (Campbell et al., 2018; Piazzesi et al., 2018), thus attenuating the sarcomere length–dependent myosin-induced effect on thin-filament activation. Our recent study of XB binding and force production in myocardial fibers from RBM20-deficient mice showed that increased compliance of titin suppresses maximal tension development, reduced Ca^{2+} sensitivity, and slowed XB detachment rate due to slowed dissociation of ADP from strongly bound XBs (Pulcastro et al., 2016). This finding, and cooperative regulatory mechanisms therein, also suggests that there may be critical contributions to this LDA response due to changes in myosin kinetics or even myosin recruitment differences (i.e., strong XB binding) that vary with filament or XB compliance (Tanner et al., 2012; Fenwick et al., 2017). The observed slow XB detachment induced by the increased titin compliance may be expected to lead to more steady-state structural contributions to thin-filament activation from strongly bound XBs. In contrast, however, our current studies show that increased titin compliance blunted the strong XB effects on the conformation of N-cTnC opening to activate thin filaments.

Other alternative mechanisms may involve myosin binding protein C (MyBP-C) and/or potentially a direct troponin–myosin interaction. As an important regulatory protein of myofilaments, MyBP-C has been suggested to activate the thin filament via a direct interaction with actin/tropomyosin through its N terminus (Kulikovskaya et al., 2003; Razumova et al., 2006; Shaffer et al., 2009; Kensler et al., 2011; Bezold et al., 2013; Harris et al., 2016), which may be sarcomere length dependent. Recent evidence indicates that myosin can directly interact with troponin in vitro (Schoffstall et al., 2011; Ghashghaee and Li et al., 2017) and in vivo (Agianian et al., 2004; Perz-Edwards et al., 2011) forming a so-called "troponin bridge," which may also be sarcomere length dependent (Ait Mou et al., 2008). The nature of sarcomere length dependence among such mechanisms would provide explanations for the observed blunting effect of low titin strain on sarcomere length–induced conformational change of N-cTnC.

In summary, the present findings combined with previous results support the hypothesis that titin-based passive tension plays an important role in sarcomere LDA of the myocardium. It also provides novel evidence that the compliance of titin, and thus the passive tension of myocardium, can modulate length-dependent Ca^{2+}-troponin regulation via altering the degree of strongly bound XB binding. Further study is needed to understand the exact mechanism of how the compliance of titin synergizes with strong XB to modulate Ca^{2+}-troponin regulation in the myocardium.

Acknowledgments

This research was supported by American Heart Association grant 17GRNT33460153 (W.-J. Dong), National Institutes of Health grants R01HL80186 (W.-J. Dong), R01HL118524 and HL115988 (H. Granzier), and PO1HL624026 (R.J. Solaro), American Heart Association grant 17SDG33370153 (B.C.W. Tanner), and National Science Foundation grant 1656450 (B.C.W. Tanner).

The authors declare no competing financial interests.

Author contributions: K.-L. Li, M. Methawasin, B.C.W. Tanner, H. Granzier and W.-J. Dong carried out experimental design and performance and data analysis. All authors contributed to writing the manuscript.

Richard L. Moss served as guest editor.

Submitted: 17 August 2018
Accepted: 1 November 2018

References

Agianian, B., U. Krzic, F. Qiu, W.A. Linke, K. Leonard, and B. Bullard. 2004. A troponin switch that regulates muscle contraction by stretch instead of calcium. *EMBO J.* 23:772–779. https://doi.org/10.1038/sj.emboj.7600097

Ait Mou, Y., J.-Y. le Guennec, E. Mosca, P.P. de Tombe, and O. Cazorla. 2008. Differential contribution of cardiac sarcomeric proteins in the myofibrillar force response to stretch. *Pflugers Arch.* 457:25–36. https://doi.org/10.1007/s00424-008-0501-x

Ait-Mou, Y., K. Hsu, G.P. Farman, M. Kumar, M.L. Greaser, T.C. Irving, and P.P. de Tombe. 2016. Titin strain contributes to the Frank-Starling law of the heart by structural rearrangements of both thin- and thick-filament proteins. *Proc. Natl. Acad. Sci. USA.* 113:2306–2311. https://doi.org/10.1073/pnas.1516732113

Arteaga, G.M., K.A. Palmiter, J.M. Leiden, and R.J. Solaro. 2000. Attenuation of length dependence of calcium activation in myofilaments of transgenic mouse hearts expressing slow skeletal troponin I. *J. Physiol.* 526:541–549. https://doi.org/10.1111/j.1469-7793.2000.t01-1-00541.x

Bezold, K.L., J.F. Shaffer, J.K. Khosa, E.R. Hoye, and S.P. Harris. 2013. A gain-of-function mutation in the M-domain of cardiac myosin-binding protein-C increases binding to actin. *J. Biol. Chem.* 288:21496–21505. https://doi.org/10.1074/jbc.M113.474346

Campbell, K.S. 2011. Impact of myocyte strain on cardiac myofilament activation. *Pflugers Arch.* 462:3–14. https://doi.org/10.1007/s00424-011-0952-3

Campbell, K.S., P.M.L. Janssen, and S.G. Campbell. 2018. Force-dependent recruitment from the myosin off state contributes to length-dependent activation. *Biophys. J.* 115:543–553. https://doi.org/10.1016/j.bpj.2018.07.006

Cazorla, O., Y. Wu, T.C. Irving, and H. Granzier. 2001. Titin-based modulation of calcium sensitivity of active tension in mouse skinned cardiac myocytes. *Circ. Res.* 88:1028–1035. https://doi.org/10.1161/hh1001.090876

Chandra, M., V.L. Rundell, J.C. Tardiff, L.A. Leinwand, P.P. De Tombe, and R.J. Solaro. 2001. Ca(2+) activation of myofilaments from transgenic mouse hearts expressing R92Q mutant cardiac troponin T. *Am. J. Physiol. Heart Circ. Physiol.* 280:H705–H713. https://doi.org/10.1152/ajpheart.2001.280.2.H705

Chandra, M., M.L. Tschirgi, I. Rajapakse, and K.B. Campbell. 2006. Troponin T modulates sarcomere length-dependent recruitment of cross-bridges in cardiac muscle. *Biophys. J.* 90:2867–2876. https://doi.org/10.1529/biophysj.105.076950

Chandra, M., M.L. Tschirgi, S.J. Ford, B.K. Slinker, and K.B. Campbell. 2007. Interaction between myosin heavy chain and troponin isoforms modulate cardiac myofiber contractile dynamics. *Am. J. Physiol. Regul. Integr. Comp. Physiol.* 293:R1595–R1607. https://doi.org/10.1152/ajpregu.00157.2007

de Tombe, P.P., R.D. Mateja, K. Tachampa, Y. Ait Mou, G.P. Farman, and T.C. Irving. 2010. Myofilament length dependent activation. *J. Mol. Cell. Cardiol.* 48:851–858. https://doi.org/10.1016/j.yjmcc.2009.12.017

Dong, W.J., J. Xing, M. Villain, M. Hellinger, J.M. Robinson, M. Chandra, R.J. Solaro, P.K. Umeda, and H.C. Cheung. 1999. Conformation of the regulatory domain of cardiac muscle troponin C in its complex with cardiac troponin I. *J. Biol. Chem.* 274:31382–31390. https://doi.org/10.1074/jbc.274.44.31382

Dong, W.J., J.J. Jayasundar, J. An, J. Xing, and H.C. Cheung. 2007. Effects of PKA phosphorylation of cardiac troponin I and strong crossbridge on conformational transitions of the N-domain of cardiac troponin C in regulated thin filaments. *Biochemistry.* 46:9752–9761. https://doi.org/10.1021/bi700574n

Fabiato, A., and F. Fabiato. 1979. Calculator programs for computing the composition of the solutions containing multiple metals and ligands used for experiments in skinned muscle cells. *J. Physiol. (Paris).* 75:463–505.

Farman, G.P., E.J. Allen, K.Q. Schoenfelt, P.H. Backx, and P.P. de Tombe. 2010. The role of thin filament cooperativity in cardiac length-dependent calcium activation. *Biophys. J.* 99:2978–2986. https://doi.org/10.1016/j.bpj.2010.09.003

Feest, E.R., F. Steven Korte, A.Y. Tu, J. Dai, M.V. Razumova, C.E. Murry, and M. Regnier. 2014. Thin filament incorporation of an engineered cardiac troponin C variant (L48Q) enhances contractility in intact cardiomyocytes from healthy and infarcted hearts. *J. Mol. Cell. Cardiol.* 72:219–227. https://doi.org/10.1016/j.yjmcc.2014.03.015

Fenwick, A.J., A.M. Wood, and B.C.W. Tanner. 2017. Effects of cross-bridge compliance on the force-velocity relationship and muscle power output. *PLoS One.* 12:e0190335. https://doi.org/10.1371/journal.pone.0190335

Fitzsimons, D.P., and R.L. Moss. 1998. Strong binding of myosin modulates length-dependent Ca^{2+} activation of rat ventricular myocytes. *Circ. Res.* 83:602–607. https://doi.org/10.1161/01.RES.83.6.602

Fuchs, F., and D.A. Martyn. 2005. Length-dependent Ca(2+) activation in cardiac muscle: Some remaining questions. *J. Muscle Res. Cell Motil.* 26:199–212. https://doi.org/10.1007/s10974-005-9011-z

Fuchs, F., and Y.P. Wang. 1996. Sarcomere length versus interfilament spacing as determinants of cardiac myofilament Ca2+ sensitivity and Ca2+ binding. *J. Mol. Cell. Cardiol.* 28:1375–1383. https://doi.org/10.1006/jmcc.1996.0129

Fuchs, F., and Y.P. Wang. 1997. Length-dependence of actin-myosin interaction in skinned cardiac muscle fibers in rigor. *J. Mol. Cell. Cardiol.* 29:3267–3274. https://doi.org/10.1006/jmcc.1997.0552

Fukuda, N., Y. Wu, G. Farman, T.C. Irving, and H. Granzier. 2003. Titin isoform variance and length dependence of activation in skinned bovine cardiac muscle. *J. Physiol.* 553:147–154. https://doi.org/10.1113/jphysiol.2003.049759

Fukuda, N., Y. Wu, G. Farman, T.C. Irving, and H. Granzier. 2005. Titin-based modulation of active tension and interfilament lattice spacing in skinned rat cardiac muscle. *Pflugers Arch.* 449:449–457. https://doi.org/10.1007/s00424-004-1354-6

Fukuda, N., T. Terui, I. Ohtsuki, S. Ishiwata, and S. Kurihara. 2009. Titin and troponin: Central players in the Frank-Starling mechanism of the heart. *Curr. Cardiol. Rev.* 5:119–124. https://doi.org/10.2174/157340309788166714

Fukuda, N., T. Terui, S. Ishiwata, and S. Kurihara. 2010. Titin-based regulations of diastolic and systolic functions of mammalian cardiac muscle. *J. Mol. Cell. Cardiol.* 48:876–881. https://doi.org/10.1016/j.yjmcc.2009.11.013

Fusi, L., E. Brunello, Z. Yan, and M. Irving. 2016. Thick filament mechano-sensing is a calcium-independent regulatory mechanism in skeletal muscle. *Nat. Commun.* 7:13281. https://doi.org/10.1038/ncomms13281

Ghashghaee, N.B., K.L. Li, et al. 2017. Direct interaction between troponin and myosin enhances the ATPase activity of heavy meromyosin. *Biologia.* 72:702–708. https://doi.org/10.1515/biolog-2017-0079

Gordon, A.M., and E.B. Ridgway. 1987. Extra calcium on shortening in barnacle muscle. Is the decrease in calcium binding related to decreased cross-bridge attachment, force, or length? *J. Gen. Physiol.* 90:321–340. https://doi.org/10.1085/jgp.90.3.321

Granzier, H.L., and S. Labeit. 2006. The giant muscle protein titin is an adjustable molecular spring. *Exerc. Sport Sci. Rev.* 34:50–53. https://doi.org/10.1249/00003677-200604000-00002

Güth, K., and J.D. Potter. 1987. Effect of rigor and cycling cross-bridges on the structure of troponin C and on the Ca^{2+} affinity of the Ca^{2+}-specific regulatory sites in skinned rabbit psoas fibers. *J. Biol. Chem.* 262:13627–13635.

Hannon, J.D., D.A. Martyn, and A.M. Gordon. 1992. Effects of cycling and rigor crossbridges on the conformation of cardiac troponin C. *Circ. Res.* 71:984–991. https://doi.org/10.1161/01.RES.71.4.984

Harris, S.P., B. Belknap, R.E. Van Sciver, H.D. White, and V.E. Galkin. 2016. C0 and C1 N-terminal Ig domains of myosin binding protein C exert different effects on thin filament activation. *Proc. Natl. Acad. Sci. USA.* 113:1558–1563. https://doi.org/10.1073/pnas.1518891113

Hoffman, R.M., T.M. Blumenschein, and B.D. Sykes. 2006. An interplay between protein disorder and structure confers the Ca2+ regulation of striated muscle. *J. Mol. Biol.* 361:625–633. https://doi.org/10.1016/j.jmb.2006.06.031

Irving, T., Y. Wu, T. Bekyarova, G.P. Farman, N. Fukuda, and H. Granzier. 2011. Thick-filament strain and interfilament spacing in passive muscle: Effect of titin-based passive tension. *Biophys. J.* 100:1499–1508. https://doi.org/10.1016/j.bpj.2011.01.059

Kensler, R.W., J.F. Shaffer, and S.P. Harris. 2011. Binding of the N-terminal fragment C0-C2 of cardiac MyBP-C to cardiac F-actin. *J. Struct. Biol.* 174:44–51. https://doi.org/10.1016/j.jsb.2010.12.003

Kobirumaki-Shimozawa, F., T. Inoue, S.A. Shintani, K. Oyama, T. Terui, S. Minamisawa, S. Ishiwata, and N. Fukuda. 2014. Cardiac thin filament regulation and the Frank-Starling mechanism. *J. Physiol. Sci.* 64:221–232. https://doi.org/10.1007/s12576-014-0314-y

Kolb, J., F. Li, M. Methawasin, M. Adler, Y.N. Escobar, J. Nedrud, C.T. Pappas, S.P. Harris, and H. Granzier. 2016. Thin filament length in the cardiac sarcomere varies with sarcomere length but is independent of titin and nebulin. *J. Mol. Cell. Cardiol.* 97:286–294. https://doi.org/10.1016/j.yjmcc.2016.04.013

Konhilas, J.P., T.C. Irving, and P.P. de Tombe. 2002. Myofilament calcium sensitivity in skinned rat cardiac trabeculae: Role of interfilament spacing. *Circ. Res.* 90:59–65. https://doi.org/10.1161/hh0102.102269

Konhilas, J.P., T.C. Irving, B.M. Wolska, E.E. Jweied, A.F. Martin, R.J. Solaro, and P.P. de Tombe. 2003. Troponin I in the murine myocardium: Influence on length-dependent activation and interfilament spacing. *J. Physiol.* 547:951–961. https://doi.org/10.1113/jphysiol.2002.038117

Kulikovskaya, I., G. McClellan, J. Flavigny, L. Carrier, and S. Winegrad. 2003. Effect of MyBP-C binding to actin on contractility in heart muscle. *J. Gen. Physiol.* 122:761–774. https://doi.org/10.1085/jgp.200308941

Lee, E.J., J. Peng, M. Radke, M. Gotthardt, and H.L. Granzier. 2010. Calcium sensitivity and the Frank-Starling mechanism of the heart are increased in titin N2B region-deficient mice. *J. Mol. Cell. Cardiol.* 49:449–458. https://doi.org/10.1016/j.yjmcc.2010.05.006

Lehrer, S.S. 2011. The 3-state model of muscle regulation revisited: Is a fourth state involved? *J. Muscle Res. Cell Motil.* 32:203–208. https://doi.org/10.1007/s10974-011-9263-8

Lehrer, S.S., and M.A. Geeves. 2014. The myosin-activated thin filament regulatory state, M^{-}-open: A link to hypertrophic cardiomyopathy (HCM). *J. Muscle Res. Cell Motil.* 35:153–160. https://doi.org/10.1007/s10974-014-9383-z

Li, K.-L., D. Rieck, R.J. Solaro, and W. Dong. 2014. In situ time-resolved FRET reveals effects of sarcomere length on cardiac thin-filament activation. *Biophys. J.* 107:682–693. https://doi.org/10.1016/j.bpj.2014.05.044

Li, K.L., N.B. Ghashghaee, R.J. Solaro, and W. Dong. 2016. Sarcomere length dependent effects on the interaction between cTnC and cTnI in skinned papillary muscle strips. *Arch. Biochem. Biophys.* 601:69–79. https://doi.org/10.1016/j.abb.2016.02.030

Li, M.X., L. Spyracopoulos, and B.D. Sykes. 1999. Binding of cardiac troponin-I147-163 induces a structural opening in human cardiac troponin-C. *Biochemistry.* 38:8289–8298. https://doi.org/10.1021/bi9901679

Liao, R., C.K. Wang, and H.C. Cheung. 1992. Time-resolved tryptophan emission study of cardiac troponin I. *Biophys. J.* 63:986–995. https://doi.org/10.1016/S0006-3495(92)81685-5

Linari, M., E. Brunello, M. Reconditi, L. Fusi, M. Caremani, T. Narayanan, G. Piazzesi, V. Lombardi, and M. Irving. 2015. Force generation by skeletal muscle is controlled by mechanosensing in myosin filaments. *Nature.* 528:276–279. https://doi.org/10.1038/nature15727

Mamidi, R., K.S. Gresham, and J.E. Stelzer. 2014. Length-dependent changes in contractile dynamics are blunted due to cardiac myosin binding protein-C ablation. *Front. Physiol.* 5:461. https://doi.org/10.3389/fphys.2014.00461

Mateja, R.D., M.L. Greaser, and P.P. de Tombe. 2013. Impact of titin isoform on length dependent activation and cross-bridge cycling kinetics in rat skeletal muscle. *Biochim. Biophys. Acta.* 1833:804–811. https://doi.org/10.1016/j.bbamcr.2012.08.011

Maytum, R., S.S. Lehrer, and M.A. Geeves. 1999. Cooperativity and switching within the three-state model of muscle regulation. *Biochemistry.* 38:1102–1110. https://doi.org/10.1021/bi981603e

McKillop, D.F., and M.A. Geeves. 1993. Regulation of the interaction between actin and myosin subfragment 1: Evidence for three states of the thin filament. *Biophys. J.* 65:693–701. https://doi.org/10.1016/S0006-3495(93)81110-X

Methawasin, M., K.R. Hutchinson, E.J. Lee, J.E. Smith III, C. Saripalli, C.G. Hidalgo, C.A. Ottenheijm, and H. Granzier. 2014. Experimentally increasing titin compliance in a novel mouse model attenuates the Frank-Starling mechanism but has a beneficial effect on diastole. *Circulation.* 129:1924–1936. https://doi.org/10.1161/CIRCULATIONAHA.113.005610

Moss, R.L., M. Razumova, and D.P. Fitzsimons. 2004. Myosin crossbridge activation of cardiac thin filaments: Implications for myocardial function in health and disease. *Circ. Res.* 94:1290–1300. https://doi.org/10.1161/01.RES.0000127125.61647.4F

Nagueh, S.F., G. Shah, Y. Wu, G. Torre-Amione, N.M. King, S. Lahmers, C.C. Witt, K. Becker, S. Labeit, and H.L. Granzier. 2004. Altered titin expression, myocardial stiffness, and left ventricular function in patients with dilated cardiomyopathy. *Circulation.* 110:155–162. https://doi.org/10.1161/01.CIR.0000135591.37759.AF

Neagoe, C., M. Kulke, F. del Monte, J.K. Gwathmey, P.P. de Tombe, R.J. Hajjar, and W.A. Linke. 2002. Titin isoform switch in ischemic human heart disease. *Circulation.* 106:1333–1341. https://doi.org/10.1161/01.CIR.0000029803.93022.93

Perz-Edwards, R.J., T.C. Irving, B.A. Baumann, D. Gore, D.C. Hutchinson, U. Kržič, R.L. Porter, A.B. Ward, and M.K. Reedy. 2011. X-ray diffraction evidence for myosin-troponin connections and tropomyosin movement during stretch activation of insect flight muscle. *Proc. Natl. Acad. Sci. USA.* 108:120–125. https://doi.org/10.1073/pnas.1014599107

Piazzesi, G., M. Caremani, M. Linari, M. Reconditi, and V. Lombardi. 2018. Thick filament mechano-sensing in skeletal and cardiac muscles: A common mechanism able to adapt the energetic cost of the contraction to the task. *Front. Physiol.* 9:736. https://doi.org/10.3389/fphys.2018.00736

Pulcastro, H.C., P.O. Awinda, M. Methawasin, H. Granzier, W. Dong, and B.C. Tanner. 2016. Increased titin compliance reduced length-dependent contraction and slowed cross-bridge kinetics in skinned myocardial strips from Rbm20ΔRRM mice. *Front. Physiol.* 7:322. https://doi.org/10.3389/fphys.2016.00322

Radke, M.H., J. Peng, Y. Wu, M. McNabb, O.L. Nelson, H. Granzier, and M. Gotthardt. 2007. Targeted deletion of titin N2B region leads to diastolic dysfunction and cardiac atrophy. *Proc. Natl. Acad. Sci. USA.* 104:3444–3449. https://doi.org/10.1073/pnas.0608543104

Razumova, M.V., J.F. Shaffer, A.Y. Tu, G.V. Flint, M. Regnier, and S.P. Harris. 2006. Effects of the N-terminal domains of myosin binding protein-C in an in vitro motility assay: Evidence for long-lived cross-bridges. *J. Biol. Chem.* 281:35846–35854. https://doi.org/10.1074/jbc.M606949200

Reconditi, M., M. Caremani, F. Pinzauti, J.D. Powers, T. Narayanan, G.J. Stienen, M. Linari, V. Lombardi, and G. Piazzesi. 2017. Myosin filament activation in the heart is tuned to the mechanical task. *Proc. Natl. Acad. Sci. USA.* 114:3240–3245. https://doi.org/10.1073/pnas.1619484114

Rieck, D., and W.-J. Dong. 2014. Conformational States and Behavior of the Heterotrimeric Troponin Complex Troponin: Regulator of Muscle Contraction. J.-P. Jin. Nova Biomedical, New York. 91–126.

Rieck, D.C., K.-L. Li, Y. Ouyang, R.J. Solaro, and W.J. Dong. 2013. Structural basis for the in situ Ca(2+) sensitization of cardiac troponin C by positive feedback from force-generating myosin cross-bridges. *Arch. Biochem. Biophys.* 537:198–209. https://doi.org/10.1016/j.abb.2013.07.013

Schoffstall, B., V.A. LaBarbera, N.M. Brunet, B.J. Gavino, L. Herring, S. Heshmati, B.H. Kraft, V. Inchausti, N.L. Meyer, D. Moonoo, et al. 2011. Interaction between troponin and myosin enhances contractile activity of myosin in cardiac muscle. *DNA Cell Biol.* 30:653–659. https://doi.org/10.1089/dna.2010.1163

Shaffer, J.F., R.W. Kensler, and S.P. Harris. 2009. The myosin-binding protein C motif binds to F-actin in a phosphorylation-sensitive manner. *J. Biol. Chem.* 284:12318–12327. https://doi.org/10.1074/jbc.M808850200

Smith, L., C. Tainter, M. Regnier, and D.A. Martyn. 2009. Cooperative cross-bridge activation of thin filaments contributes to the Frank-Starling mechanism in cardiac muscle. *Biophys. J.* 96:3692–3702. https://doi.org/10.1016/j.bpj.2009.02.018

Sun, Y.B., F. Lou, and M. Irving. 2009. Calcium- and myosin-dependent changes in troponin structure during activation of heart muscle. *J. Physiol.* 587:155–163. https://doi.org/10.1113/jphysiol.2008.164707

Tachampa, K., H. Wang, G.P. Farman, and P.P. de Tombe. 2007. Cardiac troponin I threonine 144: Role in myofilament length dependent activation. *Circ. Res.* 101:1081–1083. https://doi.org/10.1161/CIRCRESAHA.107.165258

Tanner, B.C., T.L. Daniel, and M. Regnier. 2012. Filament compliance influences cooperative activation of thin filaments and the dynamics of force production in skeletal muscle. *PLOS Comput. Biol.* 8:e1002506. https://doi.org/10.1371/journal.pcbi.1002506

Trombitás, K., A. Redkar, T. Centner, Y. Wu, S. Labeit, and H. Granzier. 2000. Extensibility of isoforms of cardiac titin: Variation in contour length of molecular subsegments provides a basis for cellular passive stiffness diversity. *Biophys. J.* 79:3226–3234. https://doi.org/10.1016/S0006-3495(00)76555-6

Trombitás, K., Y. Wu, D. Labeit, S. Labeit, and H. Granzier. 2001. Cardiac titin isoforms are coexpressed in the half-sarcomere and extend independently. *Am. J. Physiol. Heart Circ. Physiol.* 281:H1793–H1799. https://doi.org/10.1152/ajpheart.2001.281.4.H1793

Wu, Y., O. Cazorla, D. Labeit, S. Labeit, and H. Granzier. 2000. Changes in titin and collagen underlie diastolic stiffness diversity of cardiac muscle. *J. Mol. Cell. Cardiol.* 32:2151–2161. https://doi.org/10.1006/jmcc.2000.1281

Xing, J., J.J. Jayasundar, Y. Ouyang, and W.J. Dong. 2009. Förster resonance energy transfer structural kinetic studies of cardiac thin filament deactivation. *J. Biol. Chem.* 284:16432–16441. https://doi.org/10.1074/jbc.M808075200

Zhang, X., T. Kampourakis, Z. Yan, I. Sevrieva, M. Irving, and Y.B. Sun. 2017. Distinct contributions of the thin and thick filaments to length-dependent activation in heart muscle. *eLife.* 6:6.